

Dynamics of Morphology-Dependent Resonances by Openness in Dielectric Disk for TE polarization

Jinhang Cho, Sunghwan Rim, and Chil-Min Kim

Acceleration Research Center for Quantum Chaos Applications, Sogang University, Seoul 121-742, Korea

We have studied the parametric-evolution of morphology-dependent resonances according to the change of openness in a two-dimensional dielectric microdisk for TE polarization. For the first time, we report that the dynamics exhibits avoided resonance crossings between inner and outer resonances even though the corresponding billiard is integrable. Due to these recondite avoidances, inner and outer resonances can be exchanged and Q -factor of inner resonances is strongly affected. We analyze the diverse phenomena arisen from the dynamics including the avoided crossings.

PACS numbers: 42.25.-p, 42.55.Sa, 05.45.Mt

I. INTRODUCTION

Morphology-dependent resonances (MDRs), which is defined as the resonances found in cylindrical, spherical and ellipsoidal shaped optical cavities, are a much studied topic in the field of optics due to their practical importance in many applications [1] as well as their heuristic value. More than a decade ago, Johnson is the first to approach MDR in a spherical cavity [2] as an analogy of quantum mechanical resonances, which is familiar in nuclear, atomic, and molecular scattering theory. By the same approach, Nöckel have studied MDR analytically in a cylindrical cavity [3] as an unperturbed system in order to analyze a slightly deformed one.

Recently, study of the MDR is resurfaced as a hot issue in connection with the application of deformed microcavity lasers because of its high potentiality of application for photonics and optoelectronics. Bogomolny *et al.* have reported the existence of a different set of resonances, which can be classified as shape (*outer*) resonances (*ORs*) with high leakage along with Feshbach (*inner*) resonances (*IRs*) in a two-dimensional dielectric circular microdisk for transverse magnetic (TM) and transverse electric (TE) polarizations [4, 5]. The similar topic was treated in a numerical method for quantum billiard [6]. The evolutions of these two classes of resonances to the so-called *small opening limit* where the refractive index n of the disk goes to infinity have been explicitly studied [7] and the applicability of effective potential analogy for the ORs has been checked [8]. One intriguing fact of the MDR dynamics from last two studies is that, for TE polarization with magnetic field \vec{H} perpendicular to the cavity plane, both IRs and ORs are found in the same region of complex wavenumber plane where the regime of n is practically relevant.

In two-dimensional chaotic quantum billiards, it is well known that the level dynamics resembles dynamics of one-dimensional particles with repulsive interaction as a system parameter varies [9]. It is called avoided level crossing. Similarly, avoided resonance crossing (ARC) phenomenon in open Hamiltonian systems is generally categorized into two classes [10]. In the case of a strong interaction, shortly *strong ARC*, the imaginary

parts of complex-valued energies are crossing and the real parts are avoided. The identities of the two modes are exchanged via the ARC and their wave patterns are strongly superposed during the ARC. For a weak interaction, shortly *weak ARC*, the real parts are crossing and the imaginary parts are avoided while their identities are retained.

In two-dimensional chaotic dielectric cavities, there have been undertaken many theoretical [11–16] and experimental [17–19] researches related with the ARC. Due to the open property, the resonance dynamics in a dielectric cavity is much complicated and shows diverse aspects compared to that of the closed billiard. Recently, it has been represented that, when a deformation parameter is varied in the rectangular or elliptic cavity, of which the corresponding billiard is integrable, ARC can occur by the effect of openness [20, 21].¹ Another recent report have claimed that, even on a slight deformation from the disk shape, a symmetry breaking of escaping rays occurs, which gives rise to dramatic changes in emission patterns depending on the characteristics of deformations [22], and emission directions and resonance patterns are deeply influenced by the refractive index of the cavity, i.e., openness of the system, as well as the underlying classical manifold structures [23]. These imply that analyzing the emission directions and mode patterns of slightly deformed cavities requires understanding of the MDR dynamics for openness.

In this paper, we uncover the mechanism behind the MDR dynamics in a circular disk for TE polarization as the openness parameter $\Omega = 1/n$ is varied and observe the impacts of pure openness on the dynamics. The perfect rotational symmetry provides the analysis possible.

¹ In the pure one-dimensional system like a double-well potential, integrability does not forbid avoided crossing between two states.

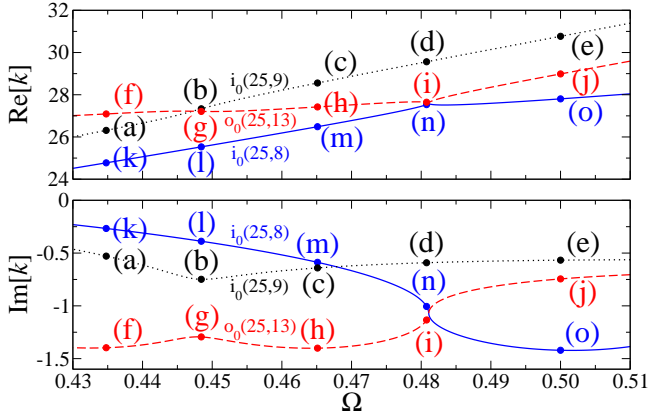


FIG. 1: (Color online) ARCs between IR and low-leaky OR. Solid, dotted, and dashed lines are $i_0(25, 8)$, $i_0(25, 9)$, and $o_0(25, 13)$, respectively.

II. AVOIDED RESONANCE CROSSINGS IN DIELECTRIC DISK FOR TE POLARIZATION

The generic two-dimensional dielectric cavities have mainly two types of changeable system parameters, e.g., degree of geometrical deformation and openness. In such cavities, IRs can generally interact with each other. Their resonance dynamics contains a complicated mixture of the aspect by deformation and the effect of openness. On the other hand, the circular disk does not have any deformation parameter and the only relevant parameter is the openness. Moreover, its rotational symmetry makes that the angular component of the wavefunction is trivial. As a result, it renders the system effectively one-dimensional and then leads more clear and basic study for the pure openness without the aspect by deformation.

The Helmholtz equation of dielectric cavities is given by $\nabla^2\psi + (k/\Omega)^2\psi = 0$, where ψ and k are the wavefunction and the wavenumber, respectively. In the disk with the radius $R = 1$, the complex-valued wavenumbers k_r for resonances are obtained from the boundary matching conditions for TM and TE polarizations under the purely outgoing wave condition [24, 25]. In the opening regime $0 < \Omega < 1$, the IRs, $i(m, l)$, are labelled by angular momentum quantum number m and modal ordering number l which corresponds to the number of radial intensity peaks inside the cavity. Similarly, the ORs can be also represented by $o(m, l)$, where l is assigned in accordance with the increasing order of $\text{Re}[k_r]$. For a given m , the maximum numbers of ORs in TM and TE polarizations are $\lfloor \frac{m}{2} \rfloor$ and $\lfloor \frac{m+1}{2} \rfloor$, respectively (the notation $\lfloor \cdot \rfloor$ is integer value). Notice that, in TE case, some ORs have relatively low leakage and we have especially called them *low-leaky outer resonances* (low-leaky ORs) [8]. Since there is only one low-leaky OR having the largest $\text{Re}[k_r]$ among the ORs for each $m (> 0)$, low-leaky ORs can be denoted by $o(m, \lfloor \frac{m+1}{2} \rfloor)$. Additionally, the notations $i_0(m, l)$ and $o_0(m, l)$ are used for IR and OR in the small opening limit, respectively, where they can

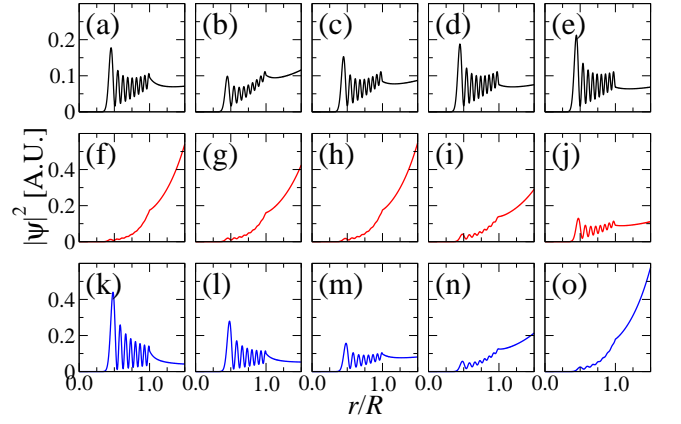


FIG. 2: (Color online) Metamorphosis of two IRs and a low-leaky OR. Top, middle, and bottom rows are $i_0(25, 9)$, $o_0(25, 13)$, and $i_0(25, 8)$, respectively. Five pictures in each row are at $\Omega = 0.435, 0.448, 0.465, 0.481$, and 0.500 .

be unambiguously identified [7, 8]. The subscript zero means $\Omega \rightarrow 0$.

When $o_0(m, \lfloor \frac{m+1}{2} \rfloor)$ is evolved from the small opening limit toward the large opening regime, both weak ARC and strong ARC are unexpectedly observed in the dielectric disk. Figure 1 shows the two types of ARCs between IR and low-leaky OR with $m = 25$. At $\Omega \simeq 0.448$, $o_0(25, 13)$ interacts with $i_0(25, 9)$ via weak ARC. When the openness increases, $o_0(25, 13)$ interacts with $i_0(25, 8)$ via strong ARC at $\Omega \simeq 0.481$. The radial intensity patterns at five points on each line in Fig. 1 are shown in Fig. 2. Due to the superposition near the point of the weak ARC at $\Omega \simeq 0.448$, the leakage of $o(25, 13)$ (Fig. 2(g)) decreases while that of $i(25, 9)$ (Fig. 2(b)) increases. However their identities are retained after the ARC as shown in Figs. 2(c) and (h). Likewise at the weak ARC, $o(25, 13)$ and $i(25, 8)$ also undergo the change of leakage and their spatial patterns are superposed near the point of strong ARC as shown in Figs. 2(h) and (m). Especially, just at the point of the strong ARC, two resonances are strongly superposed and then their patterns are almost identical as shown in Figs. 2(i) and (n). After the strong ARC, the identities of $i(25, 8)$ and $o(25, 13)$ are exchanged as shown in Figs. 2(j) and (o). Consequently, $o_0(25, 13)$ becomes $i(25, 8)$ and $i_0(25, 8)$ becomes $o(25, 13)$. On a further increase of Ω over 0.51 , $i_0(25, 8)$, which has become $o(25, 13)$, interacts with $i_0(25, 7)$ through another strong ARC. Eventually $i_0(m, l)$ can experience strong ARCs up to two times over the whole regime of Ω . $i_0(m, l)$ changes to $o(m, \lfloor \frac{m+1}{2} \rfloor)$ at the first strong ARC and $i_0(m, l)$ to $i(m, l-1)$ at the following second strong ARC:

$$i_0(m, l) \xrightarrow{\text{strong ARC}} o(m, \lfloor \frac{m+1}{2} \rfloor) \xrightarrow{\text{strong ARC}} i(m, l-1).$$

On the other hand, $i_0(25, 9)$ and $i_0(25, 8)$ do not interact each other, even if they have the same symmetry

and their imaginary values of k_r cross at $\Omega \simeq 0.468$. It has been known that two-dimensional optical dielectric cavities are typically non-integrable systems due to their open property and the openness breaks the integrability of the systems. Consequently, the avoided crossings between the IRs occur in the optical cavities, even if their corresponding billiards are integrable. It was explicitly shown in elliptic and rectangular cavity [20, 21]. But, unlike the cavities which correspond to integrable billiards such as rectangular and elliptic cavity, the avoided crossings between IRs intriguingly do not occur in the case of circular disk cavity even though the system is open. This fact implicitly indicates that the IRs remain with the properties of the normal modes in the corresponding billiard which is integrable in this case.

III. TOY MODEL

Before we discuss the numerical results, we will consider the analytical approach through a toy model. The ARCs can be displayed with effective Hamiltonian composed of a non-Hermitian 2×2 matrix and a coupling term as follows:

$$H_{\text{eff}}(\Omega) = \begin{pmatrix} E_i(\Omega) & 0 \\ 0 & E_o(\Omega) \end{pmatrix} + \begin{pmatrix} 0 & \eta\Omega \\ \xi\Omega & 0 \end{pmatrix}, \quad (1)$$

where $E_i(\Omega)$ and $E_o(\Omega)$ are the complex energy k_r^2 of IR and OR, respectively. The off-diagonal element in the coupling term, $\eta \in \mathbb{C}$ ($\xi \in \mathbb{C}$), describes the coupling effect from OR (IR) to IR (OR) and it is assumed that the coupling effects are proportional to Ω due to the fact that the coupling must become zero in the small opening limit. Equation (1) leads the eigenvalues

$$E_{\pm}(\Omega) = \frac{E_i(\Omega) + E_o(\Omega)}{2} \pm \sqrt{\frac{(E_i(\Omega) - E_o(\Omega))^2}{4} + \eta\xi\Omega^2}. \quad (2)$$

To simply illustrate the ARCs, we substitute $E_i(\Omega)$ and $E_o(\Omega)$ with the intuitive relations of the MDR dynamics. Firstly, to obtain the basic MDR dynamics for TE case except for the effects of mode interaction and Brewster angle by openness, we borrow the dynamics for TM polarization, in which the interactions between the two types of resonances are infinitesimal in the experimentally feasible opening regime due to the absence of low-leaky ORs. From this, $\text{Re}[k_r]$ and $\text{Im}[k_r]$ of an IR become almost linear to Ω and to γ , respectively [3–5]. Here, γ given by

$$\gamma = -\frac{\Omega}{2} \ln \frac{1 + \Omega}{1 - \Omega} \quad (3)$$

is the lower bound of $\text{Im}[k_r]$ of IRs in TM case. Also an OR in TM case maintains almost a constant complex valued k_r for the change of Ω [4, 5, 8]. Secondly, we consider that the destinations of nk_r of IRs and k_r of ORs in the small opening limit for TE case, correspond to

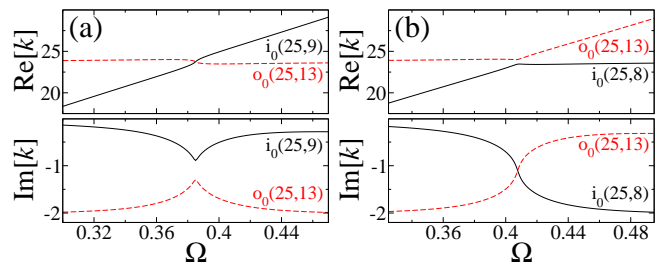


FIG. 3: (Color online) Analytical modeling of (a) weak ARC and (b) strong ARC. Solid and dashed lines are IR and OR, respectively.

the zeros of Bessel function [7, 26], $j_{m,l}$, and the zeros of Hankel function derivatives [7], $h'_{m,l}$, respectively. Then, $E_i(\Omega)$ and $E_o(\Omega)$ for TE case can be simply expressed as follows:

$$\begin{aligned} E_i(\Omega) &\approx (j_{m,l}\Omega + i\gamma)^2, \\ E_o(\Omega) &\approx (h'_{m,l})^2. \end{aligned} \quad (4)$$

Even though we borrowed the MDR dynamics for TM case, the dynamics of $\sqrt{E_i(\Omega)}$ and $\sqrt{E_o(\Omega)}$ was well matched to the numerically obtained resonance tracing behaviors [8] for TE case in the opening regime where the interaction is very small. Figures 3(a) and 3(b) show weak ARC of $i_0(25,9)$ and strong ARC of $i_0(25,8)$ with $o_0(25,13)$, respectively, when the coupling constant $\eta\xi = 12737.8$. The value of coupling constant was properly chosen as compared with the numerical result Fig. 1.

The degree of mode coupling depends on the relative quantity between $(E_i - E_o)^2$ and coupling strength $\eta\xi\Omega^2$ located in the second term of right-hand side of Eq. (2). According to the relative quantity, the crossing point of Ω are determined and the transition of the type of ARC can be occur. It is a well-known phenomenon [10, 12, 20]. In Fig. 3 obtained from the toy model, (a) is about $i_0(25,9)$ and (b) is about $i_0(25,8)$. Under the our coupling constant matched to the numerical result (Fig. 1), the point of transition from weak ARC to strong ARC for $m = 25$ is shown between these two IRs.

IV. DYNAMICS OF MORPHOLOGY-DEPENDENT RESONANCES BY OPENNESS

The dynamics from the numerical result and the toy model is explained in terms that the coupling between cavity itself and environment becomes strong as openness increases, and then the IRs are exquisitely affected by low-leaky ORs in large opening regime. Hence, a care should be taken to the identification of MDRs according to the history of ARCs. On a resonance position plot in the large opening regime, various IRs can coexist such as once and twice swapping resonances after strong ARCs,

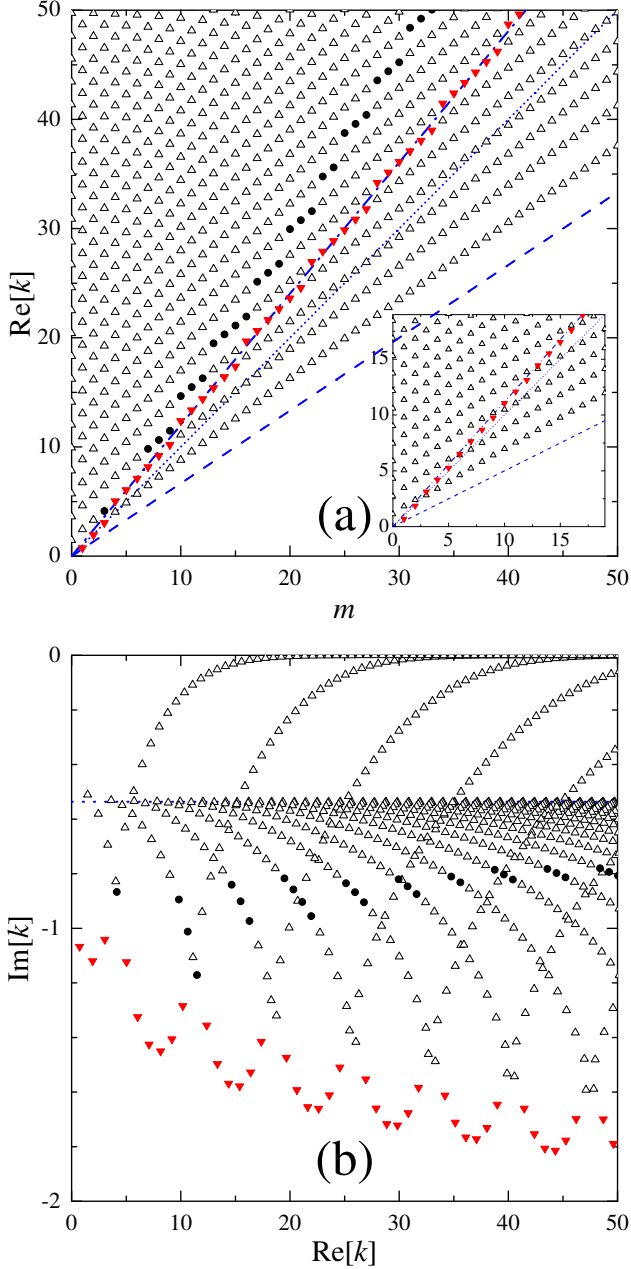


FIG. 4: (Color online) Resonance positions at $\Omega = 0.667$ for TE polarization. Inverted triangles are $o(m, \lceil \frac{m+1}{2} \rceil)$ and the others are $i(m, l)$ decided by considering ARC. Circles are $i(m, l)$ changed from $o_0(m, \lceil \frac{m+1}{2} \rceil)$. Dashed, dotted, and dot-dashed lines in (a) are $\text{Re}[k] = m\Omega$, $\text{Re}[k] = m$, and k_B , respectively. The inset in (a) is for $\Omega = 0.5$. Blue dotted line in (b) is γ .

those superposed near weak ARCs and strong ARCs, and the uncoupled ones. Figure 4 shows the resonance positions in consideration of the ARCs. We included only the IRs and the low-leaky ORs for the sake of convenience. The dotted and the dashed lines in Fig. 4(a) are $\text{Re}[k] = m$ and $\text{Re}[k] = m\Omega$, respectively. In the effective potential analogy, $\text{Re}[k] = m$ corresponds to the top of

the effective potential barrier, that is, the critical incident angle for IRs and $\text{Re}[k] = m\Omega$ corresponds to the bottom of the barrier, that is, the incident angle $\theta = \pi/2$. Effective potential analogy is successfully applied to schematic description of the properties for IRs. For this reason, it is often used on the research about the resonances in dielectric disk. We, however, note that the effective potential analogy has some insufficient parts yet on applying to ORs[8]. For a given m in Fig. 4(a), a circle is $i(m, l)$ changed from $o_0(m, \lceil \frac{m+1}{2} \rceil)$ by the first strong ARC and an inverted triangle is $o(m, \lceil \frac{m+1}{2} \rceil)$ changed from $i_0(m, l)$ by the final strong ARC. The triangles between the circle and the inverted triangle are $i(m, l-1)$ changed from $i_0(m, l)$ by two consecutive strong ARCs. If we are able to get anyhow a correct position of $o(m, \lceil \frac{m+1}{2} \rceil)$, it is natural that $i_0(m, l)$, whose $\text{Re}[k_r]$ s are positioned between $o_0(m, \lceil \frac{m+1}{2} \rceil)$ and $o(m, \lceil \frac{m+1}{2} \rceil)$, are $i(m, l-1)$ [7], because $o(m, \lceil \frac{m+1}{2} \rceil)$ must be excluded from the ordering of l for $i(m, l)$.

Here, we newly use a line number for ORs defined as $q = \lceil \frac{m+1}{2} \rceil - l$, ($q = 0, 1, 2, \dots$) and, then, the low-leaky ORs are on the line of $q = 0$. The individual line of q except zero is generally parallel to the line of $\text{Re}[k] = m$. However, the line of $q = 0$ has a different slope. It surprisingly corresponds to the Brewster angle in large opening regime. In the viewpoint of semiclassics, the incident angle for an IR can be estimated by $\sin\theta = m\Omega/\text{Re}[k]$ and the Brewster angle is represented as $\theta_B = \arctan(\Omega)$. Consequently, one can obtain $\text{Re}[k]$ relevant to the Brewster angle, that is, $k_B = m\sqrt{1 + \Omega^2}$. In Fig. 4(a) and inset, $\text{Re}[k_r]$ s of low-leaky ORs are well-aligned on the k_B line, whether they have experienced strong ARC or not. Also, by strong ARC in the opening regime where IRs and low-leaky ORs are coexistent in the same region of k plane, $\text{Im}[k_r]$ s of low-leaky ORs settle down in the bottom region of the IR group as shown in Fig 4(b).

Figure 5(a) is the three-dimensional representation of the dynamics of $i_0(25, l \leq 13)$ and $o_0(25, 13)$ in $\text{Re}[k_r]$, $\text{Im}[k_r]$ and Ω space. For more detailed depiction and notation of reference marks, we projectively plot the dynamics of $\text{Re}[k_r]$ and $\text{Im}[k_r]$ in Fig. 5(b) and Fig. 5(c), respectively. The dynamics of $\text{Re}[k_r]$ for IRs and ORs in TM polarization exhibits almost linear and constant behaviors, respectively [3–5]. On the other hand, in TE case, the low-leaky ORs breaks the monotonic behavior of IRs as shown in Fig. 5(b) through the ARCs. As Ω increases, $o_0(25, 13)$ interacts with $i_0(25, l)$, where $13 \geq l \geq 9$, sequentially through a series of weak ARCs before it interacts with $i_0(25, 8)$ through the first strong ARC at $\Omega \simeq 0.481$, i.e., there is a transition from weak ARC to strong ARC. In the large opening regime, the point of strong ARC satisfies k_B for given m and Ω , since $\text{Re}[k_r]$ s of IRs increase while $\text{Re}[k_r]$ s of low-leaky ORs tend to maintain near k_B . After the first strong ARC, $\text{Re}[k_r]$ of $i_0(25, 8)$ stays near k_B because the resonance turns to $o(25, 13)$ by the exchange of their identities. The strong ARCs between $o(25, 13)$ and $i_0(25, l)$,

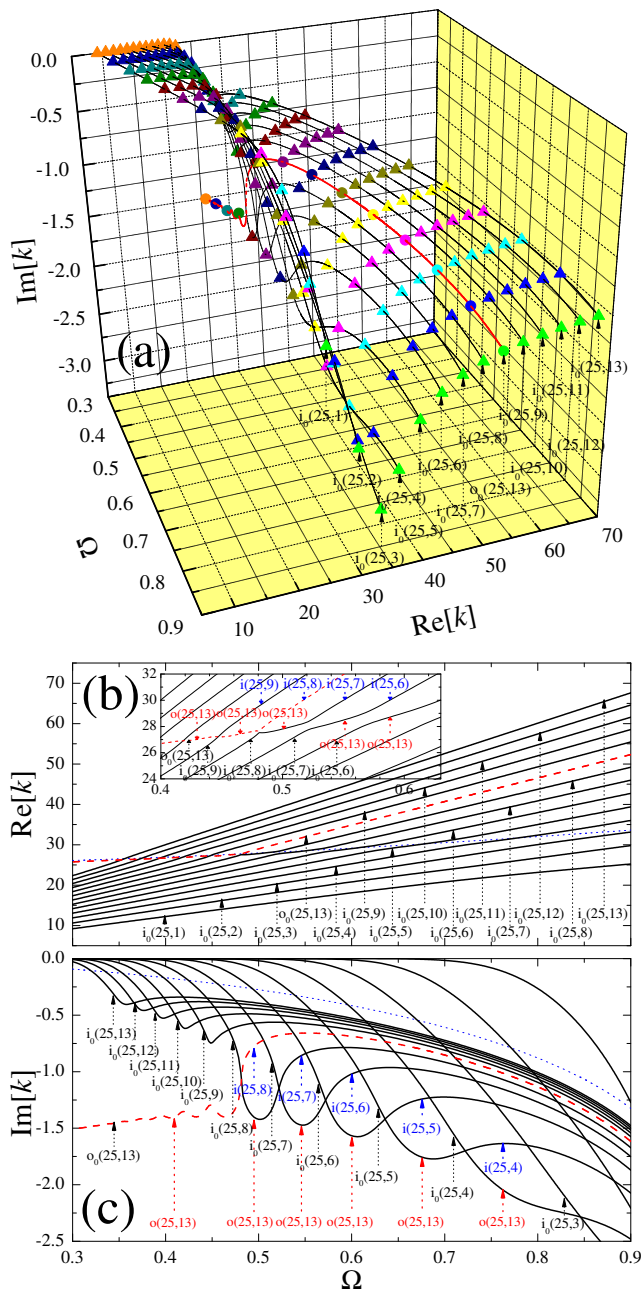


FIG. 5: (Color online) Dynamics of MDR with $m = 25$ by openness. Solid lines and a dashed line are $i_0(25, l \leq 13)$ and $o_0(25, 13)$, respectively. Dotted line in (b) and (c) is k_B and γ , respectively.

where $l \leq 8$, sequentially occur at $\text{Re}[k_r] \simeq k_B$ in the region of $\Omega \geq 0.481$ until Ω becomes unity, where all resonances merge into the continuum.

The dynamics of $\text{Im}[k_r]$ shows more interesting behavior. $\text{Im}[k_r]$ for a resonance is directly connected to the lifetime ($\tau = -1/2c\text{Im}[k]$) and Q -factor ($Q = -\text{Re}[k]/2\text{Im}[k]$). On the space of $\text{Im}[k_r]$ vs Ω as shown in Fig. 5(c), IR and low-leaky OR approach each other near the point of ARC. Since the low-leaky OR has lower

Q than the IRs for the same m , $|\text{Im}[k_r]|$ of $i(25, l)$ increases by the interaction with $o(25, 13)$. Moreover, the increased $|\text{Im}[k_r]|$ after ARC is always below the bound line γ due to the aftermath of the ARC. Hence, at a fixed value of Ω , the IRs positioned below the γ line are the resonances influenced by the ARCs. This is the reason why the IRs for TE polarization have generally lower Q than the corresponding modes for TM case [4, 5, 7, 8, 26] and their imaginary part falls below the γ line in the ordinary experimental regime of Ω as shown in Fig 4(b).

Also, the dynamics gives a clear explanation for the breaking of the decreasing order of Q -factor in accordance with the increasing order of l near the Brewster angle. In a local region of complex k space under experimentally feasible circumstances, the grouping of resonances by the order of Q makes it possible for us to predict the characteristics of the resonances. If the effects of ARC are practically zero, the IR with higher l has generally low Q according to the effective potential analogy since a resonance with higher energy is less trapped in the effective potential [2, 8, 24, 25]. In TE case, however, the order of Q of IRs is reversed from a certain value of l due to ARCs with ORs as shown in Fig. 5(c). For instance, at $\Omega = 0.5$, the order of Q corresponds to the order of l in TM case as $Q_{i(25,9)} = 85.876 > Q_{i(25,10)} = 83.253 > Q_{i(25,11)} = 82.528$. On the other hand, in TE case, the order is reversed as $Q_{i(25,9)} = 27.116 < Q_{i(25,10)} = 33.120 < Q_{i(25,11)} = 38.377$. As Ω increases, this phenomenon is extended to the resonances with lower l due to the increase of the coupling strength.

Such phenomena, only occur for TE polarization case, indicate that the existence of Brewster angle strongly activate the interactions between IRs and ORs as Ω increases. In the dielectric disk for TE polarization, the IRs are sensitively affected by Brewster angle for the internal cavity boundary. So, the IRs whose $\text{Re}[k_r]$ is near k_B have larger leakage ($|\text{Im}[k]|$) than the others [26]. i.e., the more $\text{Re}[k_r]$ of IRs approaches to k_B , the more the leakage of the IR increases. An IR whose leakage is increased near the Brewster angle by the change of openness, as Ω increases, approaches to a low-leaky OR in complex k space. Then, the coupling with the low-leaky OR becomes relatively strong and the interaction between them is more activated. Such ARC for each IR occurs sequentially at other points of Ω . Moreover, since the coupling strength becomes strong as Ω increases, the transition to strong ARC from weak ARC occurs based on an IR with specific value of l as shown in Fig. 5.

V. SUMMARY

Summarizing, we have demonstrated that the MDR dynamics by openness in a dielectric circular microdisk for TE polarization shows ARCs over two types of resonances due to the coupling with environment. The low-leaky outer resonances interact pronouncedly with the inner resonances through the opening channel near the

Brewster angle. As a result, in the opening regime relevant to experiments, the resonance classification between inner and outer resonances is more complicated and the change of leakage for inner resonances occurs. The reverse order of Q -factors of inner resonances which is discrepant from the effective potential analogy can be understood in terms of the ARCs between inner and outer resonances. This study will be useful as a basis to analyze intricate resonance dynamics in deformed dielectric microcavities.

ACKNOWLEDGMENTS

We would like to thank I. Kim, J.-W. Ryu, S.-Y. Lee, and T. Harayama for helpful discussions. This work was supported by Acceleration Research (Center for Quantum Chaos Applications) of MEST/KOSEF.

-
- [1] R.K. Chang and A.J. Campillo (Eds.), *Optical Processes in Microcavities* (World Scientific, Singapore, 1996).
- [2] B.R. Johnson, *J. Opt. Soc. Am. A* **10**, 343 (1993).
- [3] J.U. Nöckel and A.D. Stone, *Nature (London)* **385**, 45 (1997).
- [4] R. Dubertrand, E. Bogomolny, N. Djellali, M. Lebental, and C. Schmit, *Phys. Rev. A* **77**, 013804 (2008),
- [5] E. Bogomolny, R. Dubertrand, and C. Schmit, *Phys. Rev. E* **78**, 056202 (2008).
- [6] S. Tasaki, T. Harayama, and A. Shudo, *Phys. Rev. E* **56**, R13 (1997).
- [7] C.P. Dettmann, G.V. Morozov, M. Sieber, and H. Waalkens, *Europhys. Lett.* **87**, 34003 (2009).
- [8] J. Cho, I. Kim, S. Rim, G.-S. Yim, and C.-M. Kim, *Phys. Lett. A* **374**, 1893 (2010).
- [9] H.-J. Stöckmann, *Quantum Chaos* (Cambridge University Press, Cambridge, England, 2000).
- [10] W.D. Heiss, *Phys. Rev. E* **61**, 929 (2000), A.I. Magunov et al., *Physica E* **9**, 474 (2001).
- [11] J. Wiersig and M. Hentschel, *Phys. Rev. A* **73**, 031802(R) (2006).
- [12] S.-Y. Lee, J.-W. Ryu, J.-B. Shim, S.-B. Lee, S.W. Kim, and K. An, *Phys. Rev. A* **78**, 015805 (2008).
- [13] J. Wiersig, S.W. Kim, and M. Hentschel, *Phys. Rev. A* **78**, 053809 (2008).
- [14] J.-W. Ryu, S.-Y. Lee, and S.W. Kim, *Phys. Rev. A* **79**, 053858 (2009).
- [15] I. Lizuain, E. Hernández-Concepción, and J.G. Muga, *Phys. Rev. A* **79**, 065602 (2009).
- [16] C. Poli, B. Dietz, O. Legrand, F. Mortessagne, and A. Richter, *Phys. Rev. E* **80**, 035204(R) (2009).
- [17] B. Dietz, A. Heine, A. Richter, O. Bohigas, and P. Leboeuf, *Phys. Rev. E* **73**, 035201(R) (2006)
- [18] S.-B. Lee, J. Yang, S. Moon, S.-Y. Lee, J.-B. Shim, S.W. Kim, J.-H. Lee, and K. An, *Phys. Rev. A* **80**, 011802(R) (2009).
- [19] S.-B. Lee, J. Yang, S. Moon, S.-Y. Lee, J.-B. Shim, S.W. Kim, J.-H. Lee, and K. An, *Phys. Rev. Lett.* **103**, 134101 (2009).
- [20] J. Wiersig, *Phys. Rev. Lett.* **97**, 253901 (2006).
- [21] J. Unterhinninghofen, J. Wiersig, and M. Hentschel, *Phys. Rev. E* **78**, 016201 (2008).
- [22] S.C. Creagh, *Phys. Rev. Lett.* **98**, 153901 (2007).
- [23] J. Lee, S. Rim, J. Cho, and C.-M. Kim, *Phys. Rev. Lett.* **101**, 064101 (2008).
- [24] J.U. Nöckel, Ph.D. Thesis, Yale University, 1997.
- [25] M. Hentschel, Ph.D. Thesis, Max Planck Institute for the Physics of Complex Systems, 2002.
- [26] J.-W. Ryu, S. Rim, Y.-J. Park, C.-M. Kim, and S.-Y. Lee, *Phys. Lett. A* **372**, 3531 (2008).